

# Advances in Microscale Atmospheric Modeling

*J. E. Bossert (ALDTR), R. R. Linn (rrl@lanl.gov), J. M. Reisner, S. Smith, and J. Winterkamp (EES-8)*

The Atmospheric and Climate Sciences Group's recent advances in numerical modeling of small-scale phenomena in the atmosphere are based on two models, the High GRADient applications model, HIGRAD, and a physics-based wildfire-behavior model, FIRETEC. These codes have allowed us to simulate atmospheric phenomena at very high spatial resolution on LANL's supercomputers. Results from the application of HIGRAD/FIRETEC have greatly increased our physical understanding of atmospheric flows in the presence of strong heat sources and topographic obstacles. Specific examples, which are discussed below, highlight these accomplishments.

## Modeling System

The high-resolution, strong-gradient applications model, HIGRAD, solves the compressible forms of the conservation equations for mass, momentum, energy, oxygen, and other chemical species of interest in the atmosphere. HIGRAD uses numerical techniques that are fully second-order in time and space, include monotonicity constraints to handle the over- and under-shoots associated with representing strong gradients numerically, and minimize numerical diffusion that tends to diminish steep gradients with time.

Small-scale physical processes relevant to wildfires are represented in the FIRETEC combustion/turbulence-closure model. FIRETEC was developed to simulate wildfire behavior by representing the underlying physical processes that control wildfires (coupling atmospheric flows with large heat sources, mixing-limited chemical reactions, transport of reacting chemical species, etc.). FIRETEC also incorporates a turbulence transport scheme that represents the turbulence generated by the vegetation. It accounts for the microscopic details of a fire with macroscopic resolution by dividing quantities into mean and fluctuating parts similar to the approach used in traditional turbulence modeling. These divided

quantities include fuel, wind, and gas concentrations.

Combining these two models into HIGRAD/FIRETEC allows simulation of dispersion of atmospheric pollutants associated with wildfires or other sources. The numerical techniques used make HIGRAD/FIRETEC especially useful for modeling circumstances such as abrupt changes in either boundary conditions (e.g., the complex terrain of the LANL site or of an urban area—surface boundary conditions) or internal-state variable structures (e.g., strong temperature inversions in the atmosphere). Three examples of HIGRAD/FIRETEC applications are discussed below.

## Using Spatial Fuels Data to Investigate Wildfires

In one of the more interesting tests of HIGRAD/FIRETEC applied to real wildfires, we simulated a small portion of the 16,000-acre Calabasas fire that occurred on 21 to 22 October 1996 in the Santa Monica Mountains of Los Angeles County, California. Our simulation was limited to an intense fire—a blowup—that occurred in an isolated canyon around noon on 22 October. Overall, the Calabasas incident was a typical Santa Ana wind-driven conflagration that burned from Highway 101 southwestward to the Pacific Ocean

on 21 October. That night, however, the offshore winds eased, allowing residual fire lines to be affected by the normal onshore sea breeze during the morning of 22 October.

Our study area, Corral Canyon, is a north-south oriented 4-km-long watershed running between the crest of the Santa Monica Mountains (~700 m above sea level) and the Pacific Ocean. At the bottom of the canyon is a narrow riparian corridor resistant to burning. At the time of the Calabasas fire, the steep slopes of the canyon were densely covered in typical coastal chaparral vegetation.

We used AVIRIS, an aircraft-borne remote sensing spectrometer that images some 220 wavebands in the visible and near-infrared portions of the spectrum, to create the appropriate model data sets related to the spatial variability of these fuels (Figure 1). Differential analysis of reflected sunlight in these wavebands allows discrimination of surface properties, including types of ground cover and, thus, fuels.

This study constituted one of the first attempts to use the HIGRAD/FIRETEC model with both “coarse” resolution and real topography. The model resolution was 10 m in the horizontal and 5 m in the vertical—considerably coarser than our idealized fire simulations that use resolutions of 2 m or less. For computational efficiency, we stretched the vertical coordinate over

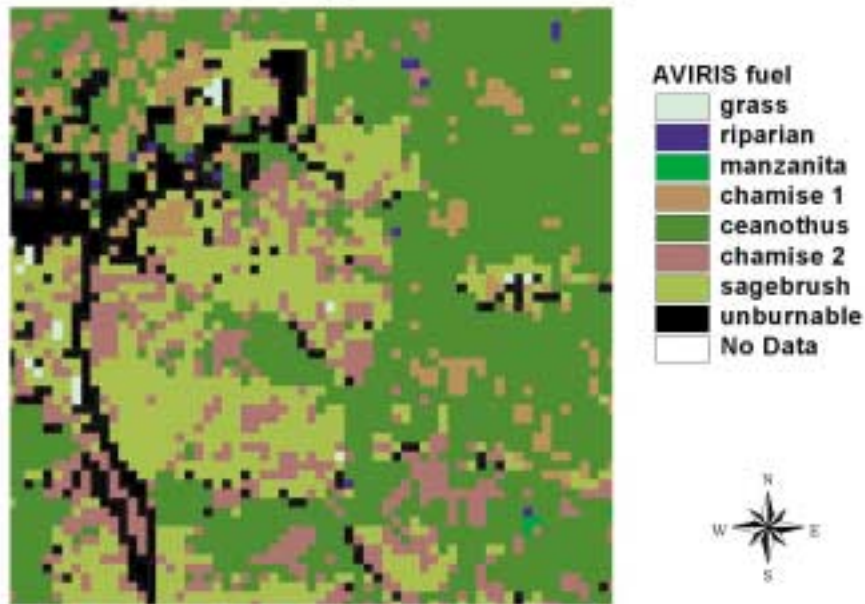


**Figure 1. Fuels in the Corral Canyon Study Area Derived from AVIRIS Data.**

The black (unburnable) area represents an asphalt road on a ridge to the west of the Malibu Bowl and housing developments on the north rim of the Bowl. The various fuel species are collectively termed "chaparral" in local terminology. The riparian corridor where the fire ignited is not shown here. This area is represented in three-dimensional perspective in Figure 2.

26 layers following a geometric progression, which established the model top at 1.3 km. The simulation domain was a 1.27-km (128-grid-cell) square, and it incorporated a topographic slice through the bottom of Corral Canyon at 10-m resolution for the lower boundary.

The Calabasas fire burned near the bottom of the canyon during the late morning of 22 October, driven by weak sea breezes. Just after noon, a fire blowup occurred on the steep slopes of the Malibu Bowl, halfway up the canyon. Several firefighters, protecting a subdivision at the top of the Bowl, were overtaken by flame lengths in excess of 100 ft during the fire blowup, and one firefighter was severely burned.

Our HIGRAD/FIRETEC simulation was able to capture many features of the actual fire behavior as related by firefighting professionals on the scene. Figure 2 shows that our simulated fire raced up the steep slopes of the Malibu Bowl after smoldering in the riparian fuel at the bottom of the canyon for 17 min

following ignition. Over the course of 15 min, our simulated fire progressed rapidly up the ridgeline at the right edge of the bowl, exactly where the firefighter, defending a home, was severely burned by the real fire. Next,

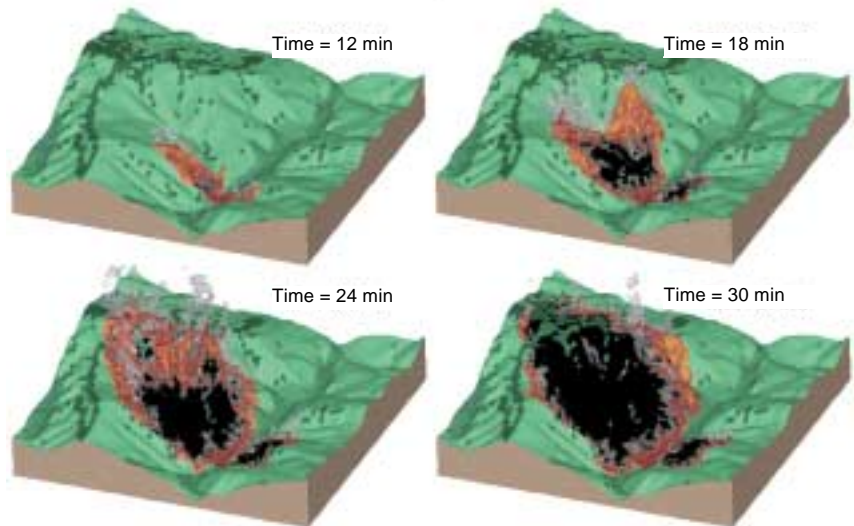


**Figure 2. FIRETEC Wildfire Simulation.**

In these snapshots, green represents unburned vegetation, black represents completely burned areas, and the other colors are keyed to model temperatures of the simulated Corral Canyon portion of the Calabasas fire. The progression of the fire in this simulation corresponds to (qualitative) observations by firefighting professionals at the scene.

our simulated fire burned out the entire Malibu Bowl in the following 5 min, exhibiting extreme behavior in terms of flame lengths, vertical velocities, and fire temperatures. Our results are consistent with observations and with the aftermath of the fire, in which the lush vegetation within the Bowl was reduced to mineral ash, indicating the intensity of the burn.

## HCl Dispersion from a Shuttle Abort Scenario

A second application of HIGRAD/FIRETEC, one that we hope will never represent real circumstances, concerns both fire and the dispersion of its combustion products. In this study, we used the combined model to examine the emissions associated with a potential catastrophic abort of a launch of the NASA Space Shuttle.

Abort procedures within the first 20 s after launch would result in an explosive fragmentation of the Shuttle's solid rocket boosters. In such a scenario, the hazards associated with emissions from the burning booster, which would produce

hydrochloric acid (HCl) gas, pose a potential exposure risk to launch visitors and nearby communities, a true cause for concern. To evaluate this potential risk, we simulated the abort scenario and analyzed the dispersion of HCl released after the rocket booster fragments reached the ground. This analysis was conducted under the guidance of the NASA Biomedical Office at the Kennedy Space Center.

To address the concerns about the potential HCl hazard, we developed a worst-case scenario that included identifying weather conditions to evaluate the predicted size and shape of the solid rocket booster debris field, the burning characteristics of the booster, and the HCl emissions and their transport. HIGRAD/FIRETEC was then used to simulate the atmosphere's response to the intense heat emitted by the burning booster fragments. We also simulated emission of HCl in the gaseous and aqueous phases in the vicinity of the shuttle launch pad and subsequent transport downstream toward the NASA causeway and Port Canaveral. To make these simulations as accurate as possible, we developed representations in HIGRAD/FIRETEC for (1) the production of heat and HCl emitted from the rocket booster fragment distribution patterns, (2) the depletion of the fragments with time, and (3) the deposition of HCl on vegetation and water surfaces.

The simulation itself was divided into two parts, each representing a different phase of the transport of HCl from the burning fragments to points of interest downwind. The first part consisted of modeling the emission of gas (HCl and other gases) and heat from the rocket fragments and the atmospheric response to these emissions. This *near-field* simulation required high resolution (~20 m) to capture the strong buoyancy-driven flows resulting from the heat released by the fragments. The physical domain for this part of the analysis

was taken to be 4.8 km along-wind by 4 km across-wind by 10 km high.

Figure 3 shows a snapshot of the HCl plume from the near-field simulation when the discrete fragment emission pattern is combined with real meteorological conditions from 23 November 1995, a day chosen to enhance our simulation of a worst case. The two features of interest are the significant amount of the plume that is trapped near the ground and between about 900 and 1,000 meters above the ground. This trapping, associated with two strong atmospheric temperature inversions at these levels, is similar to that seen in nighttime pollution episodes in urban areas.

The second part of the simulation consisted of modeling the *far-field* transport of gaseous HCl downwind after the booster fragments finished burning and the atmospheric response relaxed from the strong vertical motions associated with the burning process. To simulate this downwind transport required a larger physical domain, approximately 28 km along-wind by 12 km cross-wind by 10 km high. Consequently, we used coarser horizontal grid resolution than in the

near-field case. In the far-field simulation, it was also important to consider additional processes associated with transport of the HCl downwind, particularly the deposition of HCl onto the vegetation. Based on the initial near-field dispersion and the deposition and dilution processes in the far-field domain, we were able to conclude that HCl concentrations, even in a worst case such as we used, would be below Environmental Protection Agency (EPA) hazard levels.

### Building Flow Simulations

This third application of the HIGRAD/FIRETEC microscale atmospheric modeling system illustrates both the model's flexibility and its robust character. Although this application does not involve fire, the turbulence closures in FIRETEC play an important role in the results of this study, in which we investigate the dispersal of atmospheric contaminants within the urban environment. We focus here on the equivalent of the near-field results discussed in the last section; additional work, the

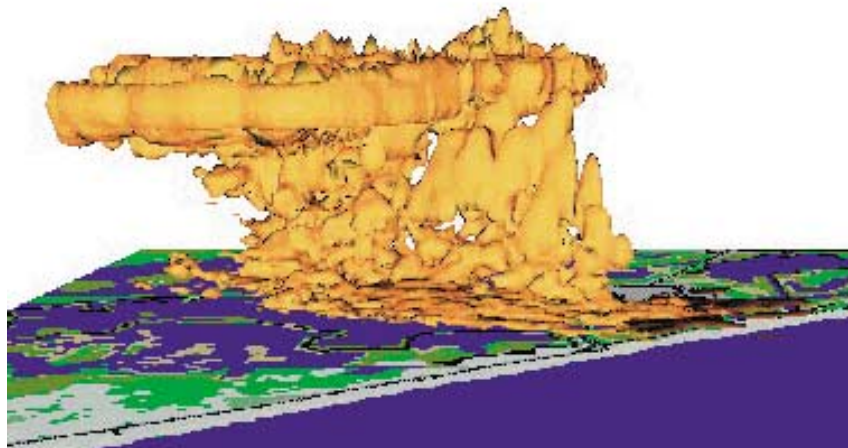


**Figure 3. Near-Field Simulation of Shuttle Abort.**

The HCl cloud is depicted using its 20-points-per-million isosurface in the near-field domain shortly after the Shuttle abort process. In this simulation, the large-scale wind field blows from right to left, spreading the cloud downwind from its ignition point (the blackened area near the "coast"). The areas of widespread HCl near the surface and at the top of the cloud are associated with temperature inversions in the meteorological conditions used.

analog of the far-field study discussed above, is in progress.

In preparation for the 2002 Winter Olympic Games to be held in Salt Lake City, Utah, we have simulated the effects of a release of an unspecified agent at the Delta Center, the Olympic skating venue. In the event of a release of a chemical or biological agent at such a large indoor event, the pollutant would diffuse throughout the interior of the building and would likely be exhausted to the atmosphere through the heating, ventilation, and air-conditioning ducts, thus exposing the population in the vicinity of the building. Our work does not concern dispersion in the interior of the Delta Center; rather, we have specified a continuous release of a passive tracer for a finite duration at the location of the air-conditioning vents as a way to investigate subsequent transport in the atmosphere outside the building.

These near-field simulations (Figure 4) use a single building on flat terrain in neutral atmospheric stratification. The dispersion shown is non-Gaussian with a substantial amount of the tracer trapped in the building recirculation zone. The concentration contours that seem unconnected with the building wake region are caused by the vents located on the upstream side and transport over the building. These results show that significant variability in concentration of hazardous agents could be located in the lee of the building for extended periods.

**Validations.** To validate these simulations and provide a basis for confidence in more complex simulations that include several buildings (the far-field case), we have compared HIGRAD/FIRETEC results with wind-tunnel experiments. These model validation runs used data obtained from a recent EPA wind-tunnel study of the flow field around a two-dimensional array of "buildings." These buildings consisted of seven evenly spaced

rectangular blocks of equal height ( $H$ ) and downwind length of 0.15 m. The spacing between each building row was  $H$ , and the building rows spanned the horizontal (cross-wind)

extent of the wind tunnel. A neutral atmospheric boundary layer was simulated in the wind tunnel by stirring the flow with spires and floor roughness elements upstream of the

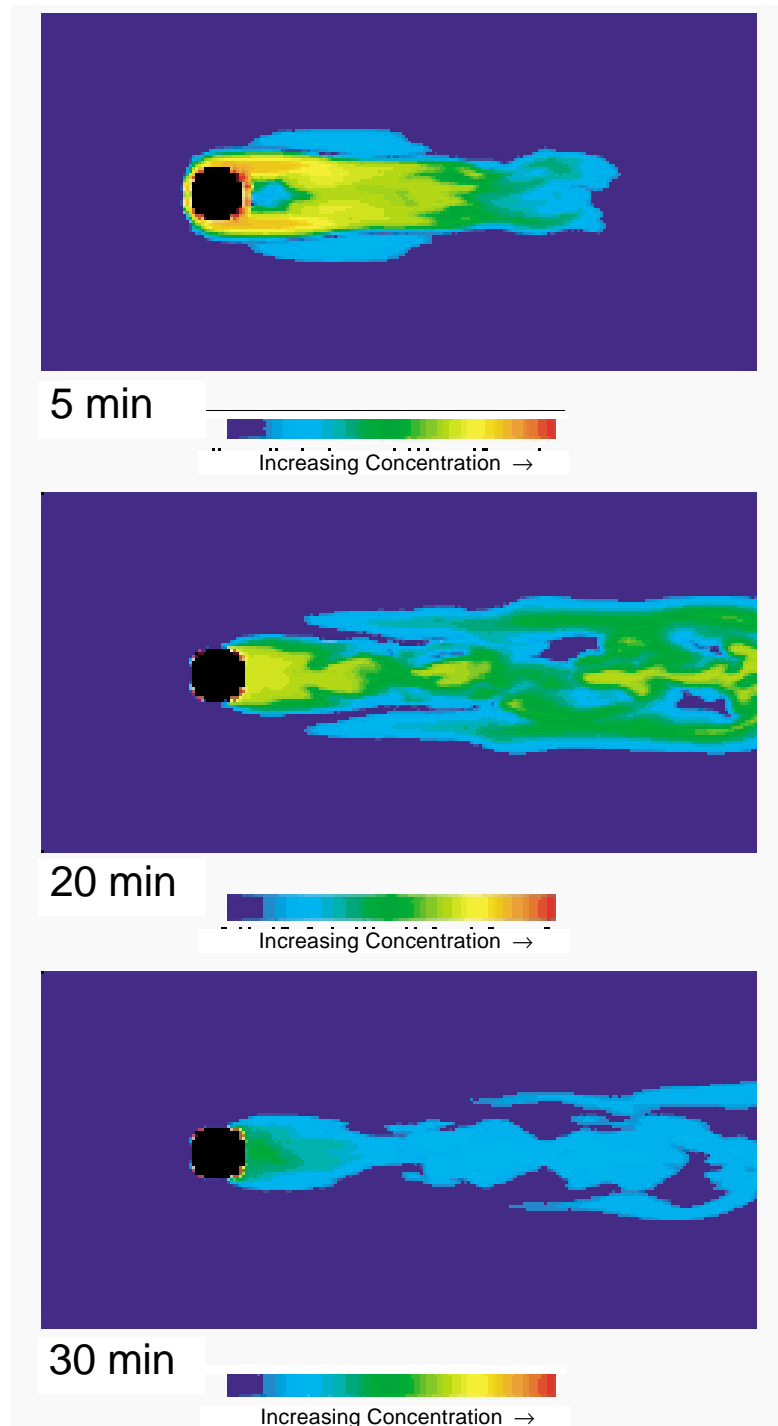


**Figure 4. Near-Field Simulation of Building Flow.**

The figure shows the transport and dispersion of pollutants downstream of a single building. Sources are located on all sides of the building, and some of the patterns here that appear unconnected to the wake are associated with transport over the building and back to the ground level.

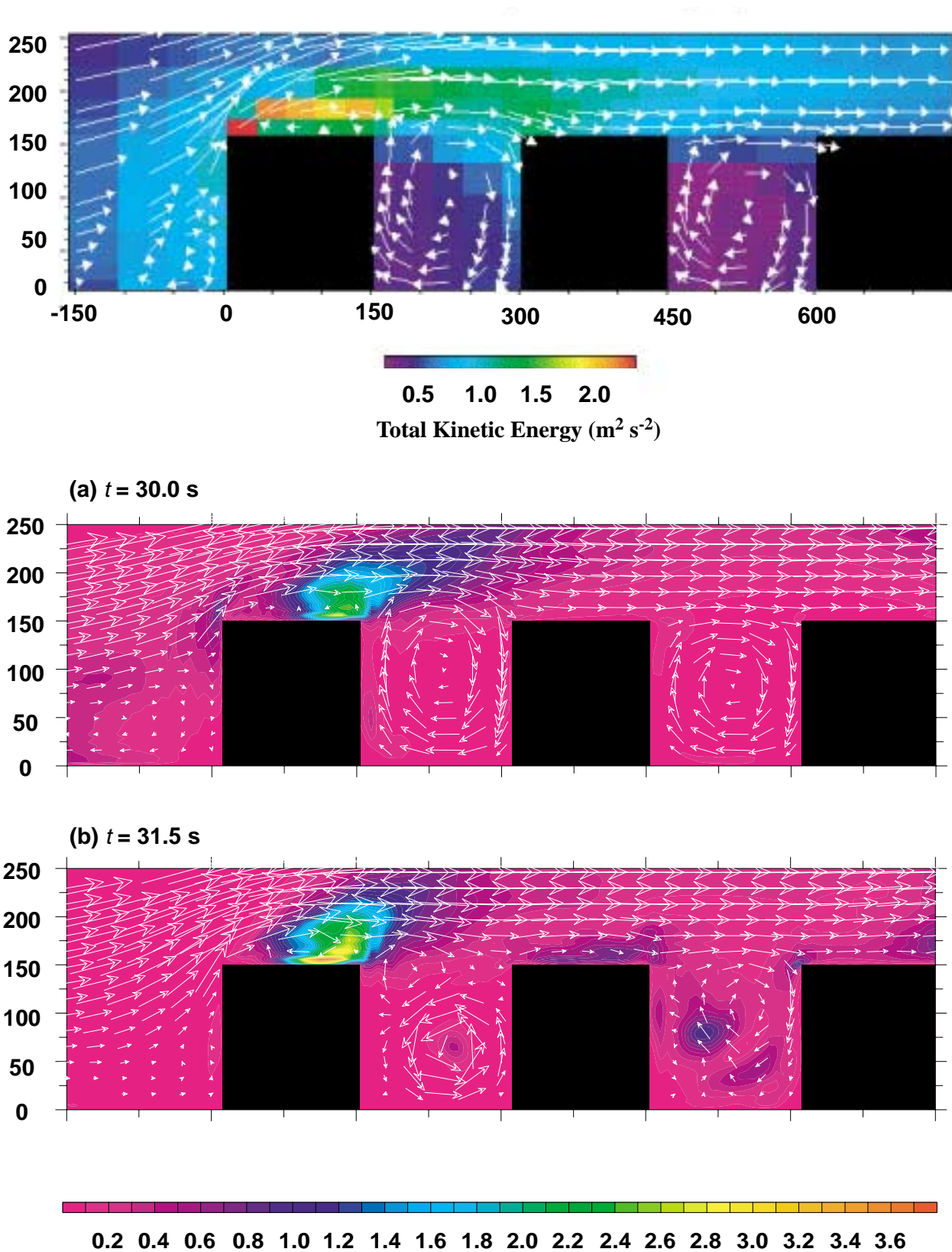


**Figure 5. Wind Tunnel and HIGRAD Simulations of Flow Over Buildings.**

The HIGRAD simulation shown here (bottom) reproduces the actual wind-tunnel geometry (top) using a downstream grid size of 1.5 cm. In addition to reproducing the overall flow pattern, HIGRAD captures such features as the structure of the turbulent kinetic energy and the flow recirculation upstream of the left-most building. (Wind-tunnel data courtesy of U.S. EPA.)

building array. High-resolution measurements of the three components of mean and turbulent velocity statistics were made with a pulsed wire anemometer at various heights within each “canyon” between the buildings, above each building, and upstream and downstream of the building array.

To simulate the wind-tunnel experiments, we used a domain size of 5.4 m in the along-flow direction and 1.4 m in the vertical direction with a  $360 \times 1 \times 51$  grid. The downwind resolution was constant, and vertical grid varied from  $0.05 H$  near the bottom of the domain to  $0.1 H$  near the top. The inflow profile of the mean velocity for the simulations was determined from the wind-tunnel data, and HIGRAD simulations were integrated for a time span of 1 min with a time increment of 0.001 s.

Figure 5 shows a crosssection down the longitudinal centerline of the observed turbulent kinetic energy and mean wind vectors, which reveals the overall flow pattern. The figure shows a flow separation and corresponding recirculation over the first building rooftop. There is no similar recirculation over the other buildings. There are well-developed clockwise rotating vortices in each of the canyons. The turbulent kinetic energy peaks at the upwind edge of the first building and is largest above the canyons. Interestingly, the modeled turbulent kinetic energy is similar to that observed turbulent kinetic energy in pattern and magnitude despite the two-dimensional nature of the simulation.

The modeled flow field matches the wind-tunnel observations reasonably well. For example, a small recirculation zone upstream of the first building is simulated, as observed in the wind tunnel study. The model simulation also reproduces the flow separation and recirculation at the top of the first building. These features are not evident for the other

buildings. Well-defined clockwise rotation in the canyons is also evident for the model simulation and wind-tunnel observations. These results have given us confidence to proceed in using the HIGRAD model as a tool to simulate urban dispersion effects for assessment and prediction purposes in real urban environments.

## Conclusions

Simulating atmospheric phenomena involves addressing processes on a wide variety of spatial scales. The discussion here is concerned with micrometeorology simulations for which computational domains of  $100 \text{ km}^2$  and less are appropriate. To simulate realistically processes associated with dispersion of contaminants and with combustion in wildfires, it is necessary to use computational techniques that can adapt to high gradients of both state variables and boundary conditions.

The LANL-developed model we call HIGRAD was designed specifically to include such gradients; in addition, it can be configured to compute the effects of the compressibility of air and the heating associated with absorption of sunlight and terrestrial radiation. This feature makes it suitable for simulating wildfires and dispersion of contaminants associated with heat sources (such as the NASA simulation discussed above) and with the complex lower boundary condition of the urban environment.

The model’s versatility is highlighted in this discussion with results from simulations on domains from 1 to  $10^8 \text{ m}^2$ . Its application to the real-world problems of wildfire and of urban dispersion is continuing and provides a full-physics benchmark for simpler parametric models. ■

## Further Reading

- Hanson, H. P., M. M. Bradley, J. E. Bossert, R. R. Linn, and L. W. Younker. 2000. The potential and promise of physics-based wildfire simulation. *Environmental Science & Policy* **3**: 161–172.
- Kao, C.-Y. J., Y.-H. Hang, D. I. Cooper, W. E. Eichinger, W. S. Smith, and J. M. Reisner. 2000. High-resolution modeling of LIDAR data mechanisms governing surface water vapor variability during SALSA. *Agricultural and Forest Meteorology* **105**: 185–194.
- Reisner, J., S. Wynne, L. Margolin, and R. Linn. 2000. Coupled atmospheric-fire modeling employing the method of averages. *Monthly Weather Review* **128**: 3683–3691.
- Reisner, J., V. Mousseau, and D. Knoll. 2001. Application of the Newton-Krylov method to geophysical flows. *Monthly Weather Review*, in press.
- Smith, W. S., J. M. Reisner, and C.-Y. J. Kao. 2001. Simulations of flow around a cubical building: Comparison with towing-tank data and assessment of radiatively-induced thermal effects. *Atmospheric Environment*, in press.